Journal of Mines, Metals and Fuels, *71(11): 2176-2184; 2023. DOI: 10.18311/jmmf/2023/36046*

Print ISSN : 0022-2755

Journal of Mines, Metals and Fuels

Contents available at: *www.informaticsjournals.com/index.php/jmmf*

Numerical Analysis of Vertical Axis Wind Turbine with Different Profiles

Pramodkumar M. Bagade[1]*, Preeti P. Bagade[2], Prabhat Ranjan[3], Amit Chakravorty[2], Eeshan Kamath[2] and Omkar Mogare[2]

[1]*Department of Mechanical Engineering, Bhivarabai Sawant College of Engineering and Research, Pune - 411041, Maharashtra, India; pramodbagade@gmail.com*

[2]*Department of Mechanical Engineering, Padmabhooshan Vasantdada Patil Institute of Technology Pune – 411021, Maharashtra; India; preetibagade10@gmail.com, amitchakravorty1997@gmail.com, kamath.eeshaan@gmail.com, omkarmogare@gmail.com*

[3]*Department of Mechanical Engineering, Shrimati Kashibai Navale College of Engineering, Pune – 411041, Maharashtra, India; prabhatiitism@gmail.com*

Abstract

Wind energy is considered to be the cleanest fuel. India is rich in natural resources; we have learned to harness them for our benefit and advancement. As a gauge of fuel demand, India's fuel consumption increased 6.5% year over year in 2023 to around 18.57 million tons, according to figures from the Petroleum Planning and Analysis Cell (PPAC). Even though it applies to all resources, we are currently focusing on harnessing wind energy. Wind turbines have been improved and researched to increase their efficiency since their inception. However, little progress was ever made on extracting wind energy lost at low wind speeds as they could not power a large commercial turbine. Vertical Axis Wind Turbines (VAWT), which typically perform better at low wind speeds. To address this issue and to increase the turbine's efficiency, we applied natural shapes and curves to the turbine design. We investigated its effects using numerical analysis, discovering that the method offers certain advantages in terms of fluid flow over the turbine body, such as having better flow over the body, a low number of vortex formations, and reduced drag effects while returning the blade to its original position.

Keywords: *Computational fluid Dynamics (CFD), Fuel, Low Wind Velocity Terrains, Vertical Axis Wind turbine, Turbine Design*

1.0 Introduction

Due to the rising cost of these fuels on the global market, using traditional fossil fuels is expensive. The cost of producing electricity from traditional power plants is rising due to the spiraling increase in fuel prices. The major challenge to use wind as a source of fuel is that it is intermittent and it does not always blow when electricity is needed. The types of wind turbines are (HAWT) and (VAWT) are employed for a variety of uses, with power production being the most prevalent. The key benefits of VAWTs are their omni-direction, the ability to directly rotate a fixed load, and their low cost. Additionally, they are scalable, have minimal manufacture, installation, and maintenance costs, and produce little noise. However, due to their more complicated unsteady aerodynamics and little attention in research for low wind speed terrains specifically, their aerodynamic performance is significantly lower than that of HAWTs; as a result, in order to benefit from their numerous advantages,

**Author for correspondence*

their aerodynamic performance also foresee further improvement. The effectiveness of VAWTs has undergone multiple efforts, and there is a resurgence of interest in wind energy harvesting in two new prospective areas, far offshore and in urban and rural settings. In both urban and rural regions, VAWTs can be positioned inside wind turbines, between buildings, and on building rooftops, catchers and ventilation ducts in both urban and rural areas. Flow phenomena include unstable separation and dynamic stall blade wake interactions, flow curvature effects, and rational impacts on boundary layers and shed vortices all have an impact on the complicated aerodynamic performance of VAWTs.

The geometrical and operational properties of the turbine are what drive such complicated processes, but by employing natural shapes for the vanes, the interaction between the wind flow and the turbine vanes is altered, leading to a new understanding of the parameters stated above.

Turbines are traditionally divided into two types: those that use drag force to rotate and those that use lift force to rotate. Researchers have also attempted to use a combination of lift and drag turbines. The former (using lift force to rotate) typically works or begins to work at higher wind speeds, which can be as high as 10mph, to begin with. In comparison, the latter (the drag-based turbine) can start at very low wind speeds but cannot harness energy at higher wind speeds and thus proves inefficient at higher wind speeds. As a result, much effort is being directed toward developing turbines capable of harnessing such low wind velocity while also operating at higher speeds. India is the only country in the world to have a dedicated ministry for renewable energy, which emphases on the cutting fuel costs by utilizing alternative sources.

All conventional wind turbines visible today operate only at high wind speeds and require a minimum wind velocity of 10m/s. Wind speeds of up to 5 m/s are common in cities. According to Betz, even a 1m^2 wind turbine can generate a theoretical maximum of 76.5 watts; in practice, at least 50 watts will be generated to power a few LED bulbs and, when combined in quantity, can easily power a house. Wind power is viewed as a mainstream electricity supply technology for the reason that it has no cost uncertainties from fuel supply price fluctuations besides other advantages. The current study employs naturally inspired shapes to capture wind energy in low-wind terrains.

2.0 Literature Review

Reza *et al.*[1] investigated a helical VAWT in the context of renewables and energy efficiency. The study was conducted in two stages: first, an analytical calculation of the power output of a helical wind turbine was completed, which then informed the design and construction of the rotor blades. Shahariar *et al.*[2] developed a theoretical model for developing and operating a Darrieus-type vertical axis wind turbine for small-scale energy applications. A small three-bladed turbine (prototype) was built, and its performance in low wind velocity was investigated. The model is based on the NACA 0018 airfoil with a light wood blade. Shah *et al.*[3] compared the rotational performances of two new Savonius rotor blade shapes to the conventional straight and curved blades.

The aerodynamic modeling, fabrication, and performance evaluation of VAWT were reported by Kalakanda *et al.*[4]. Their tests were carried out in a subsonic wind tunnel to analyze performance parameters such as power in the wind, mechanical power at the turbine shaft, Tip Speed Ratio (TSR), and power coefficient. Their rotor was tested at wind speeds ranging from 4.38 m/s to 22.38 m/s, and the designs were efficient. According to Koudad *et al.*[5], turbines must meet specific criteria, including maximum conversion of kinetic wind power to mechanical power, resistance to severe weather conditions such as storms, rain, and snow, a long lifetime, and a buzzer that is the most diminutive possible form and ensures citizens' safety. During their investigation, Yi-Xin Peng *et al.*[6] reported that Straight-Bladed Vertical-Axis Wind Turbines (SBVAWTs) have unsatisfactory power generation and self-start ability due to continuous variation of attack angle to the blades. The authors proposed that high-solidity SBVAWTs be used because of their low operational speed and good self-start performance. Kumar *et al.*[7] pointed out that HAWTs are not recognized as a viable option to yoke the energy of the wind in municipal areas, where the wind is fewer intense, greatly messier, and more turbulent. At the same time, VAWTs are recommended as a better choice for towns and isolated semi-municipal areas. Many researchers contributed to identifying problems associated with the low efficiency of VAWTs and proposed various solutions to overcome them.

Zhang *et al.*[8] obtained blades' aerodynamic coefficients through simulation and experiments of variable pitch VAWT. The authors discovered that variable-pitch VAWT improves aerodynamic performance because tangential force coefficients are twice as significant as fixed-pitch VAWT. Kanyako *et al.*[9] also preferred VAWTs for the future smart grid integration of urban wind turbines. This work creates an aerodynamic model for studying Vertical Axis Wind Turbines in low-speed environments. The authors ran a VAWT model through a 3D numerical simulation. The CFD and DMST results both showed a minutest and negative torque performance at lesser tip speed ratios for their modeled turbine, which implies the incapability of the turbine to self-start. According to Qamar *et al.*[10], The use of Vertical Axis Wind Turbines (VAWTs) is becoming more popular as a solution for problems in regions with weak winds. Understanding the ideal solution for these VAWTs is crucial to enhancing their performance. According to this study, symmetrical bladed turbines have a worse Coefficient of Performance (Cp) than VAWT with cambered blades. The turbines overcame difficult wind speed hurdles thanks to their greater Cp, which they also attained at lower tip speed ratios. In order to increase the amount of land that may be used for wind farming in the United States, Sharma *et al.*[11] discuss the high wind speeds needed by commercially viable HAWT and offer a solution in the shape of an ultra-cheap AWT that is tuned for lower average wind speeds. States. Wenchuan *et al.*[12], experimentally investigated the effect of the number of blades on the performance of a Savonius-type wind turbine model. The experiments compared 2, 3, and 4-blade wind turbines at varied Tip Speed Ratio (TSR), Torque (T), and Power Coefficient (c_p) and oncoming wind speed (V). The Savonius model with three blades performs well at a high tip speed ratio. When the wind speed is 7 m/s, the highest tip speed ratio is 0.555. When wind power is used, emissions of CO_2, SO_2, NO_x, and other hazardous wastes are virtually eliminated, unlike in conventional coal-fuel power plants or nuclear power plants that use radioactive waste. Using established hydrogen minigrid system technology, the largest wind to hydrogen power system in the UK is fuelled on wind and "green" hydrogen power[13]. According to reports, a workable stand-alone wind-diesel system can run on 50–80% less fuel than a power source that only uses diesel generation[14]. If fossil fuels are used indefinitely, the greenhouse gasses they release will cause price increases and climatic change[15,16]. Globally, researchers have extensively examined wind energy sources, biofuels, and hybrid systems as examples of renewable energy sources. In light of this, research into wind energy hybrid production will offer fresh perspectives on renewable energy sources in the future[17]. As wind electricity penetration increases, other strategies that will be more beneficial include mass market demand response, bulk energy storage technologies, large-scale electric vehicle deployment, repurposing excess wind energy for local heating or fuel production, and geographic diversification of wind power plant siting[18].

3.0 Methodology and Setup

The methodology used for the numerical analysis is shown in Figure 1 below.

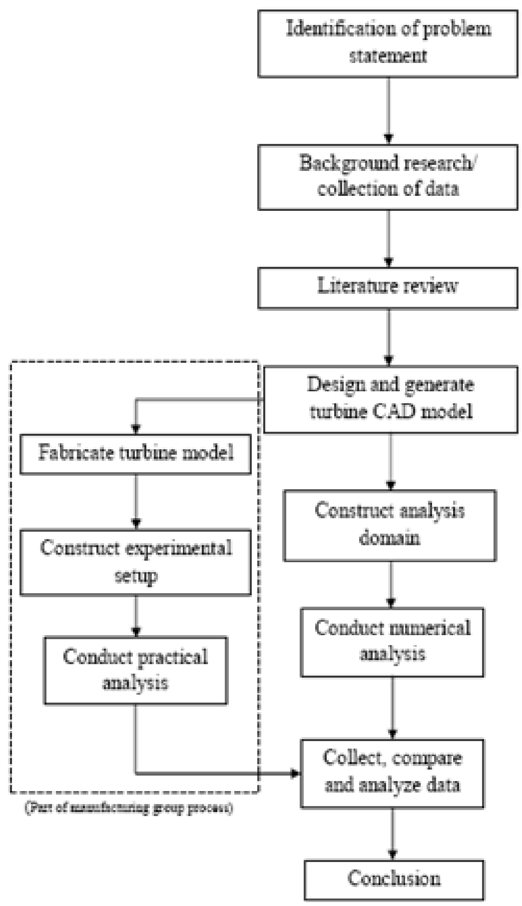

Figure 1. Flow chart for the method adopted for numerical analysis.

3.1 Simulation Setup

The turbine prototype is simulated using ANSYS FLUENT software. CATIA was used to create the CAD model, which was then exported to ANSYS Fluent for analysis. The CAD model with three blade profiles created using nature-inspired shapes is shown in Figure 2, and the schematic of the setup with boundary conditions is shown in Figure 3.

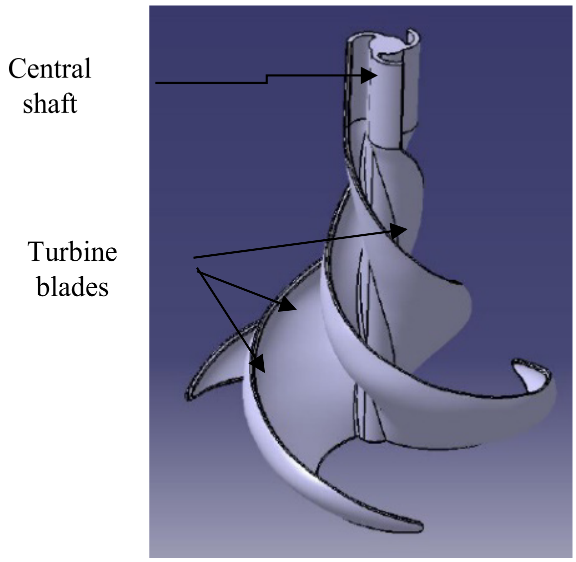

Figure 2. CAD model of turbine.

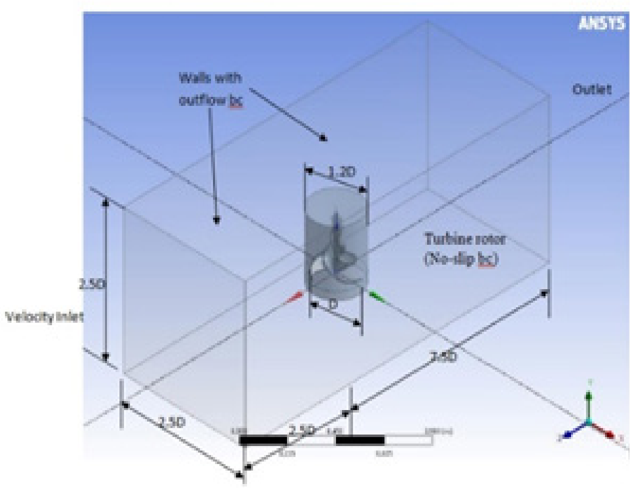

Figure 3. Schematic of the setup with boundary conditions.

The CAD model, after importing, was edited and made suitable for analysis. The edit mainly generated the fluid and rotating domains for the turbine. A flow domain of 0.8m×0.9m×2m is considered during the simulation. The rotor was enveloped in a cylinder with dimensions of 0.135m radius and 0.4m height.

3.2 Mesh

Meshing for the model was done in the meshing software provided by the ANSYS module. Parallel meshing was used for a faster meshing process. The meshing method was selected individually for the domain body and rotating or cylinder body. The domain body applied the Body Fitted Cartesian method, whereas the rotor cylinder used the Hex Dominant method. Sufficient care has been taken to take into account the grid metrics suggested by Bagade *et al.*[19]. Figure 4 shows the grid generated for the

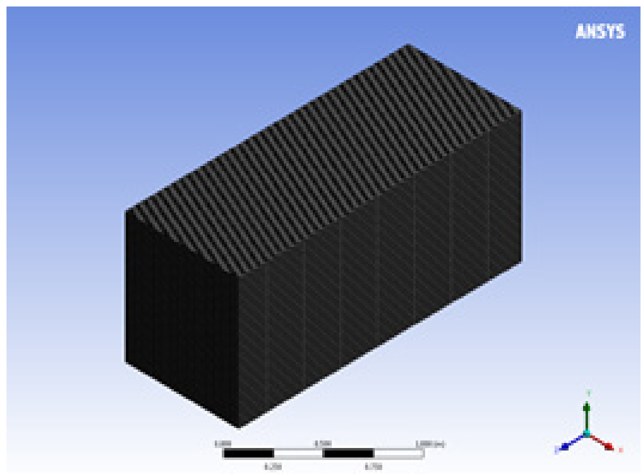

Figure 4. Overall mesh view.

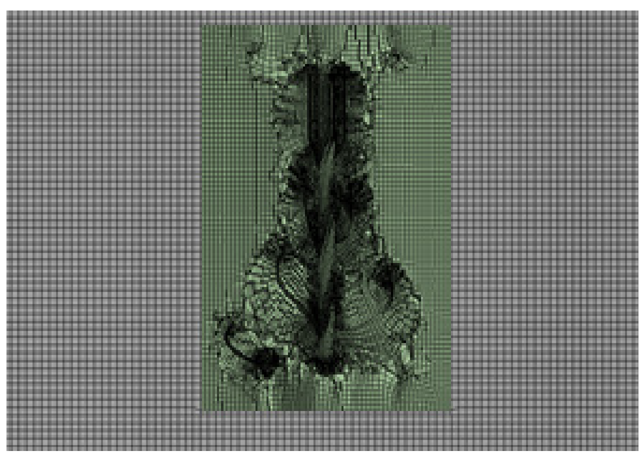

Figure 5. Mesh generated, the grey portion is the Cartesian mesh type for a domain, and the green portion is the Hex-dominant mesh type for the rotor.

Table 1. Three types of grids were tested

Grid type	Size	No. of Elements	No. of nodes
Coarse	0.8 x0.9 x 2	342158	290522
Medium	0.8 x0.9 x 2	565289	489357
Fine-I	0.8 x0.9 x 2	838595	736144
Fine-II	0.8 x0.9 x 2	985632	856337

whole domain with the fine grid. Mesh independence study was conducted with coarse and medium grids, however the details are not reported here in detail. Three types of grids were tested as follows in Table 1:

It was noted that the results with Fine-I and Fine-II grids were not changing considerably, but the computation time for Fine-II grid was considerably increased. Hence, the results were obtained with Fine-I type of grid. Figure 5 depicts Mesh generated where the grey portion is the Cartesian mesh type for a domain, and the green portion is the Hexdominant mesh type for the rotor.

3.2.1 Mesh Quality

Table 2, shows the details of the grid generated. Due to very complex geometry, orthogonality of around 0.78 was achieved. Using finer mesh resulted in higher number of nodes, which was computationally exhaustive.

Table 2. Properties, statistics, and quality of mesh

Bounding Box	
Length X	0.8 m
Length Y	0.9 m
Length Z	2. m
Properties	
Nodes	736144
Elements	838595
Mesh Metric	Orthogonal Quality
Min	1.03556×10^{-5}
Max	1
Average	0.785292019741111
Standard Deviation	0.31265039781369

Having nodes of more than 9,00,000 puts a considerable load on the available system and thus slows down the speed of the calculation process.

4.0 Results and Discussion

Figure 6, shows velocity contour of wind around turbine at t = 0 for wind velocity, V= 2m/s. At t=0.01. Potential flow solution is assumed as the initial condition.

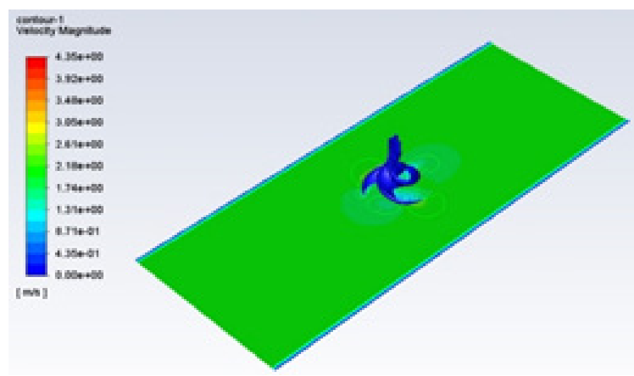

Figure 6. Velocity contour of wind around turbine at 2mps at t = 0 seconds.

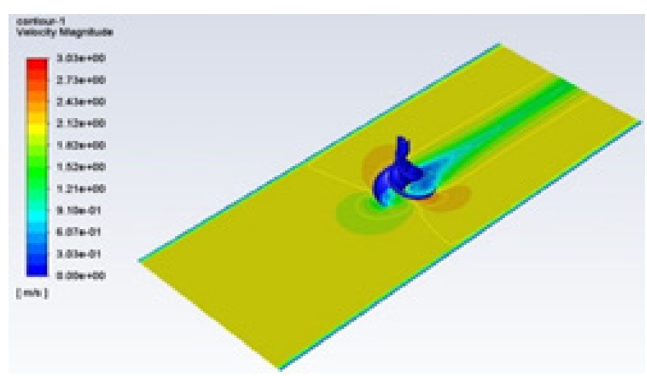

Figure 7. Velocity contour at mid-y plane at t = 5 sec for V= 2m/s.

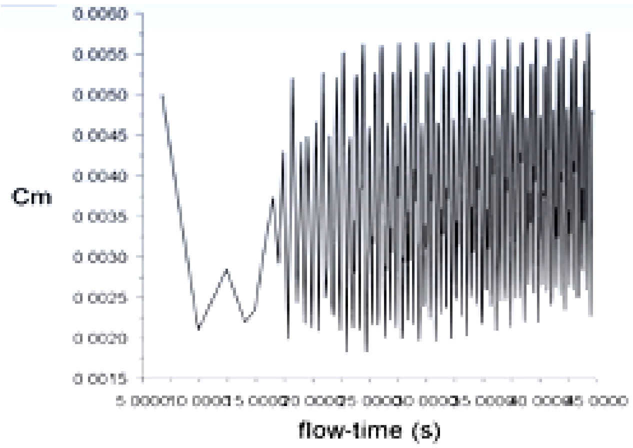

Figure 8. Graph of Cm versus time.

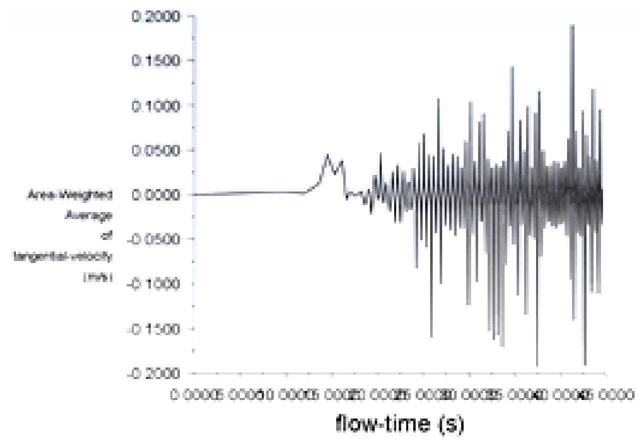

Figure 9. Evolution of tangential velocity with time.

It is noted that in the whole flow domain, a uniform velocity contour colour are seen, while at the very early time step (t = 0.01), a sign of presence of the turbine rotor is apparent. On the walls, no-slip boundary condition is applied indicating that the wind velocity on those surface regions are zero. Velocity contour at mid-y plane at t = 5 sec for V = 2m/s are shown in Figure 7. The flow is seen to be developing and a wake region is observed behind the turbine. At the tip of the blades, flow acceleration is noted, while aft-wall recirculation zone is also observed. The maximum velocity noted at this time instant was around 3 m/s, near the tip of the rotor blades.

From the contours, it is visible that the turbine body does act like a bluff body, as expected. Still, the shape of vanes and position allows the wind to reunite with the stream in a concise duration, thus reducing the area having very low wind velocity. Yet the stream behind the turbine has reduced wind velocity due to obstruction. However, his also indicates that the turbine absorbs the reduced velocity energy, which eventually results into rotation of the blades. The leading portion of the turbine shows contours of reduced velocity. In contrast, the side portion shows contours of increased velocity due to vanes acting like aerofoils. The air stream is separated, and a pressure difference is created, changing the wind velocity on both sides.

Figure 8, shows moment coefficient, Cm with time, while Figure 9 and 10 shows tangential velocity and rpm *vs.* time respectively. The coefficient of the moment shows an increasing trend even after 45 seconds, essentially indicating the increment in speed in further simulation. The oscillating patterns occur due to the rotation of the

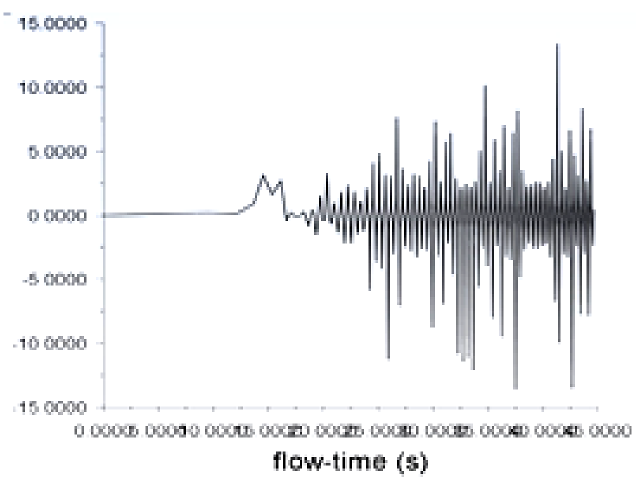

Figure 10. Rotation history (rpm) with time.

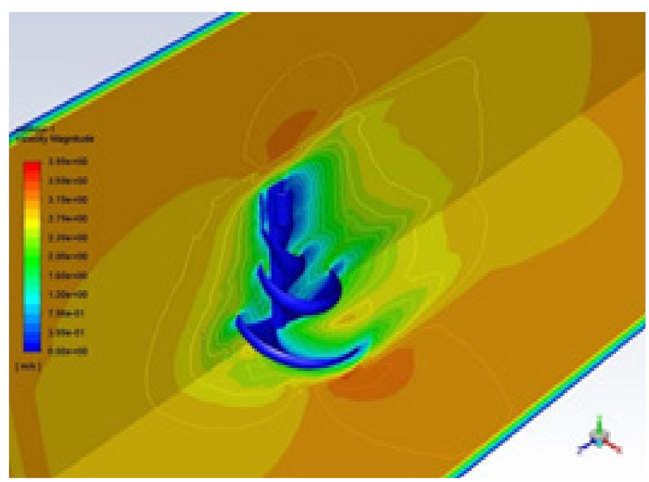

Figure 11. Velocity contour at 3m/s at t = 0.1 second.

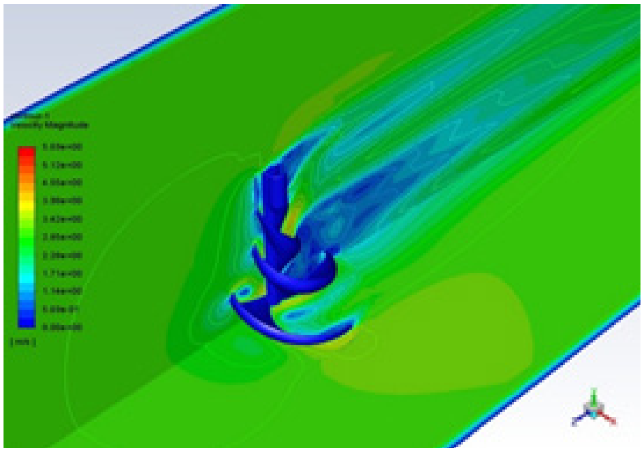

Figure 12. Velocity contour at 3 m/s at t = 1 second.

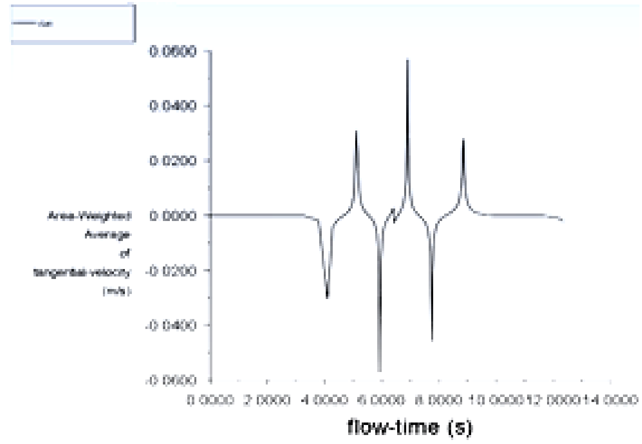

Figure 13. Tangential velocity versus time.

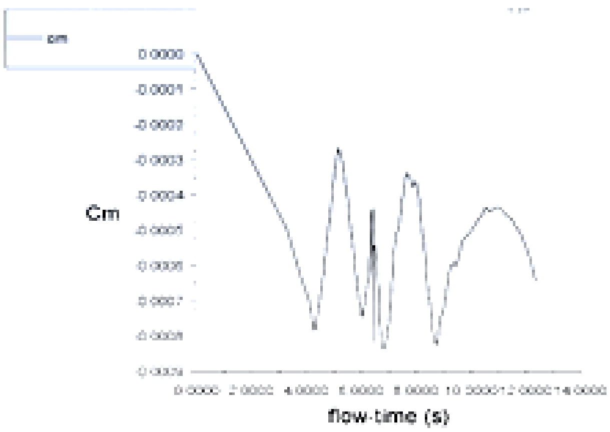

Figure 14. Cm versus time.

turbine. The faces selected for measurement of cm are the tip of the turbine vanes, with three vanes. Periodic change in forces experienced by the vane during rotation causes these broad-range oscillations in values.

Also, the increasing trend might saturate when the turbine reaches its maximum speed, but the oscillations won't stop. The value of Cm increases with an increase in turbine radius. The tangential velocity shown in Figure 9, represents the velocity at a tangential direction to the rotation of the turbine. This data corresponds to the velocity magnitude available on the turbine vane's tip during rotation. The graph gradually increases initially and is close to being called exponential rise due to its rapid increment in value. This happens because initially when the turbine is not rotating. The vanes act like a bluff body and obstruct the airflow, bringing the air velocity near zero on its face. The plot of velocity contour at 3 m/s and t = 1 second is shown in Figure 12 and flow time response has been represented in Figure 14.

The turbine starts rotating, the adjacent air molecules start moving along with it, and when the turbine vane reaches the side portion, the air is free to flow right beside it. Hence the value starts increasing at a much faster rate. And when the turbine has completed a few rotations, its speed has already improved. Hence the tangential velocity value at the tip of the turbine keeps increasing. The irregularities in the graph are caused due to the wake portions behind the turbine, through which the vane passes, causing a change in velocity magnitude due to low wind velocity portions present there.

The same mesh model was used for this analysis by changing the parameters of inlet velocity and transient time step value. Figure 11 shows velocity profiles around the turbine at t = 0.1 sec. Another plane of contour was added (mid-y and mid-z plane) to understand the flow of air over and around the turbine. It is noted that at this early time, not many high-velocity regions have developed, and the maximum value of air velocity is 3.99m/s. The rotor does not start rotating at this early time and acts as bluff body.

At t = 1 second, the flow is seen to be developing. The wake region behind the turbine is formed and more prominent than before, especially more significant than 2m/s. It is due to the higher velocity of air. The particles travel at a faster rate and thus travel farther than required after it goes over the turbine and fails to meet the airflow from the other side at a short distance.

The turbine is yet to start rotating, but its unique vanes allow the flow of air to travel in a different direction than it was traveling to. The vane after the vane visible in front carries the wind to the rear portion of the turbine. The presence of the adjacent blade results in unsteady wake creating a favorable pressure zone.

Time evolution of the tangential velocity is shown in Figure 13. This data corresponds to the velocity magnitude available on the turbine vane's tip during rotation. It is noted that velocity magnitude gradually increases initially following an exponential rise till t = 5sec. This is followed by a sudden dip in the velocity magnitude. But when the turbine starts rotating, the adjacent air molecules start moving along with it, and when the turbine vane reaches the side portion, the air is free to flow right beside it. Hence the value starts increasing at a much faster rate. And when the turbine has completed a few rotations, its speed is noted to increase. The irregularities in the graph are caused due to the wake portions behind the turbine, through which the vane passes, causing a change in velocity magnitude due to low wind velocity portions present there. The flow indicates huge aerodynamic unsteadiness in the present case.

The coefficient of the moment shows a decreasing trend even after 12 seconds, essentially indicating the increment in speed in further simulation. The oscillating patterns occur due to the rotation of the turbine. The faces selected for measurement of C_m are the tip of the turbine vanes, with three vanes. Periodic change in forces experienced by the vane during rotation causes these broad-range oscillations in values. The value has a negative nature, but because the direction of the moment is opposite to its sign conventions, only the magnitude is considered. Also, the decreasing trend might saturate when the turbine reaches its maximum speed, but the oscillations won't stop. The value of C_m increases with an increase in turbine radius.

5.0 Conclusions

The current turbine design does offer lesser drag force during the rotation of the vane to its original position against the flow of wind. But it has comparatively less efficiency due to high unsteadiness. Also at the early time steps, the rotor assembly acts as a bluff body, which indicates that there is need to investigate the profile further from aerodynamic point of view. The turbine rotates at wind velocities as low as 2m/s. It has a disadvantage in that the overall surface area of the turbine is comparatively less than a Savonius turbine of the same dimension. Small changes in design can help the turbine achieve higher efficiency than the present value. Wind energy significantly lessens reliance on fossil fuels, which are prone to price and supply volatility, hence increasing global energy security by diversifying the energy mix. Wind power is a clean, green energy source, in contrast to fossil fuels, which release toxic gasses into the atmosphere[13].

The present results provide an insight on understanding the fluid flow over a turbine based on Archimedes' spiral. Upon developing the project further and having high-fidelity data on the wind flow around it and its working, it could form a possible base for the new branch of wind turbines. It is also noted from the present study that the presence of three-dimensional Archimedean spiral vanes enhances the vanes' performance.

6.0 Acknowledgements

The present research work has been supported by the Department of Science and Technology, Science and Engineering Research Board, Government of India (Grant No. EEQ/2019/000450). The authors sincerely acknowledge the PVPIT, Pune for support received during this work.

7.0 References

1. Raza P, Mishra P, Mishra R. Aerodynamic Modeling and Analysis of Vertical Axis Wind Turbine. IJARIIE. 2019; 5(4):359-71
2. Shahariar GMH, Hasan MR. Design and construction of a vertical axis wind turbine. The 9th International Forum on Strategic Technology (IFOST). IEEE Cox's Bazar, Bangladesh. 2014; pp. 326-9. https://doi.org/10.1109/IFOST.2014.6991132
3. Shah SR, Kumar R, Raahemifar K, Fung AS. Design, modeling and economic performance of a vertical axis wind Turbine. Energy Reports. 2018; 4:619-23. https://doi.org/10.1016/j.egyr.2018.09.007
4. Kalakanda AS, Nallapaneni MK. Vertical axis wind turbine: Aerodynamic modelling and its testing in wind

tunnel. Procedia Computer Science. 2016; 93:1017-23. https://doi.org/10.1016/j.procs.2016.07.305

5. Koudad S, Mahmoudi H, Menzhi LEL. Mechanical study of a vertical axis wind turbine rotor design. International Symposium on Power Electronics, Electrical Drives, Automation and Motion (IEEE). 2016; pp. 570-4. https://doi.org/10.1109/SPEEDAM.2016.7525996
6. Peng Y-X, Xu YL, Zhan S, K. Shum KM. High-solidity straight-bladed vertical axis wind turbine: Aerodynamic force measurements. Journal of Wind Engineering and Industrial Aerodynamics. 2019; 184:34-48. https://doi.org/10.1016/j.jweia.2018.11.005
7. Kumar MS, Krishnan AS, Vijayanandh R. Vibrational Fatigue Analysis of NACA 63215 Small Horizontal Axis Wind Turbine blade. Materials Today: Proceedings. 2018; 5:6665-74. https://doi.org/10.1016/j.matpr.2017.11.323
8. Zhang X, Xu D, Liu Y. Intelligent control for large-scale variable speed variable pitch wind turbines. J Control Theory Appl. 2004; 2:305-11. https://doi.org/10.1007/s11768-004-0015-9
9. Kanyako F, Janajreh I. Vertical Axis Wind Turbine performance prediction for low wind speed environment. IEEE Innovations in Technology Conference, Warwick, RI, USA. 2014; pp. 1-10. https://doi.org/10.1109/InnoTek.2014.6877366
10. Qamar SB, Janajreh I. A comprehensive analysis of solidity for cambered darrieus VAWTs. International Journal of Hydrogen Energy. 2017; 42(30):19420-31. https://doi.org/10.1016/j.ijhydene.2017.06.041
11. Sharma KK, Biswas A, Gupta R. Performance Measurement of a Three-Bladed Combined Darrieus-Savonius Rotor. International Journal of Renewable Energy Research. 2013; 3(4): 885-91
12. Wenehenubun F, Saputra A, Sutanto H. An experimental study on the performance of Savonius wind turbines related with the number of blades. Energy Procedia. 2015; 68:297-304. https://doi.org/10.1016/j.egypro.2015.03.259
13. Tong W. Fundamentals of wind energy. WIT Transactions on State of the Art in Science and Engineering. 2010; 44:3-48. https://doi.org/10.2495/978-1-84564-205-1/01
14. Danvest Energy. Wind-diesel instructions, http://www.danvest.com/filesfordownload/wind-diesel.pdf
15. Yin Z, Zhu L, Li S, Hu T, Chu R, Mo F, Hu D, Liu C, Li Bin. A comprehensive review on cultivation and harvesting of microalgae for biodiesel production: Environmental pollution control and future directions. Bioresour Technol. 2020; 301:122804 https://doi.org/10.1016/j.biortech.2020.122804 PMid:31982297
16. Sheng Y, Mathimani T, Brindhadevi K, Basha S, Elfasakhany A, Xia C, Pugazhendhi A. Combined effect of CO_2 concentration and low-cost urea repletion/starvation in Chlorella vulgaris for ameliorating growth metrics, total and non-polar lipid accumulation and fatty acid composition. Sci Total Environ. 2022; 808:151969 https://doi.org/10.1016/j.scitotenv.2021.151969 PMid:34843758
17. Gani EA, Mamat R, Mahidin, Sudhakar K, Rosdi SM, Husin H. Biomass and wind energy as sources of renewable energy for a more sustainable environment in Indonesia: A review. Archives of Environmental Protection. 2022; 48(3):57-69
18. Wiser R, Yang Z, Hand M, Hohmeyer O, Infield D, Jensen PH, Nikolaev V, O'Malley M, Sinden G, Zervos A. Wind Energy. In IPCC Special Report on Renewable Energy Sources and Climate Change Mitigation Cambridge University Press, Cambridge, United Kingdom and New York, NY, USA. 2011 https://doi.org/10.1017/CBO9781139151153.011
19. Bagade PM, Bhumkar YG, Sengupta TK. An improved orthogonal grid generation method for solving flows past highly cambered aerofoils with and without roughness elements. Computers and Fluids. 2014; 103:275-89. https://doi.org/10.1016/j.compfluid.2014.07.031